

# Optimizing energy consumption and preventing slips at the footstep planning level

Martim Brandão, Kenji Hashimoto, José Santos-Victor and Atsuo Takanishi

**Abstract**—Energy consumption and stability are two important problems for humanoid robots deployed in remote outdoor locations. In this paper we propose an extended footstep planning method to optimize energy consumption while considering motion feasibility and ground friction constraints. To do this we estimate models of energy, feasibility and slippage in physics simulation, and integrate them into a hybrid A\* search and optimization-based planner. The graph search is done in footstep position space, while timing (leg swing and double support times) and COM motion (parameterized height trajectory) are obtained by solving an optimization problem at each node. We conducted experiments to validate the obtained energy model on the real robot, as well as planning experiments showing 9 to 19% energy savings. In example scenarios, the robot can correctly plan to optimally traverse slippery patches or avoid them depending on their size and friction; and uses stairs with the most beneficial dimensions in terms of energy consumption.

## I. INTRODUCTION

Recently there has been a rising interest in robots which are able to navigate challenging outdoor and disaster environments. There, robots might have to depend on batteries and as such energy expenditure must be minimized while still avoiding falls and undesirable slips.

Our claim in this paper is that energy consumption and slippage on humanoid robots can be optimized at the footstep planning level. The motivation is that both energy and slippage are largely related to the center-of-mass dynamics, which in turn is constrained by footstep placement and timing. The fact that certain step parameters “work better” than others has been empirically included in motion planners by using heuristics such as nominal stride and postures during planning. For example, [1] uses a quadratic preference for a nominal stride length that is “safer and more stable”, and [2] uses human-inspired polynomial costs on step length, width and rotation. Ideally, to obtain optimal energy consumption realistic energy models should be estimated. Also, ground friction and not only obstacle avoidance [3], [4], [5], [1] should be considered. If friction is considered optimally, for example, walking slower on slippery terrain might be more

energy efficient than avoiding it [6]. Since both energy and friction highly depend on the forces and motion of the COM, not only footstep position but also other parameters such as timing and COM motion should be planned.

The contributions of this paper are the following: 1) We extend the notion of footstep planning to the planning of footstep placement, timing and parameterized COM motion. 2) We obtain, through physics simulation, step-based models of energy, feasibility (kinematic and dynamic) and slippage for the full-size humanoid robot WABIAN. 3) We validate the obtained energy consumption model with a subset of experiments on the real robot. 4) We integrate these models into a hybrid A\* search and optimization-based planner, decreasing energy consumption between 9 and 19% in simulated environments with stairs and very-low-friction patches.

## II. RELATED WORK

Search-based planners such as A\* [2], [7], [3] and its variants [4], [5] have been used successfully to plan obstacle free paths in both static and dynamic [3] scenarios. Recently, purely optimization-based planners have also been proposed [1], which eliminate the sub-optimal discretization problem inherent to search-based planners. While the aforementioned planners focus on finding collision-free paths, our method attempts to go one step further: computing energy optimal paths, and considering both collision and slippage.

One important step in footstep planners is to estimate whether a given stance or step is feasible or not. Some authors opt to approximate feasibility by reachability of the feet in each stance [5], while others also pre-compute volumes swept by the legs to avoid collisions [8]. In this paper we use both rough reachability intervals to discard obvious unfeasible poses, as in [5], but also learn a model of feasibility from physics simulation: where feasibility is both kinematic (joint limits) and dynamic (no falls).

Perhaps the work most related to this paper is that of Huang et. al [2], in which terrain-related and energy-related cost functions are used in A\* search to compute optimal cost plans. Inspired by human gait-analysis and biomechanics literature, they sum a set of empirical models of energy cost that are polynomial functions of step length, width and rotation. Also [7] uses a similar approach, with quadratic cost functions on sequences of footstep positions. In this paper, we use an off-the-shelf machine learning algorithm to learn a realistic energy consumption function instead of fitting it to a predefined empirical model of human walking. We also consider ground friction when planning, and since our models include step timing and rough COM motion they can

\*This work was supported by JSPS KAKENHI Grant Number 15J06497 and ImPACT TRC Program of Council for Science, Technology and Innovation (Cabinet Office, Government of Japan).

M. Brandão is with the Graduate School of Advanced Science and Engineering, Waseda University.

K. Hashimoto is with the Waseda Institute for Advanced Study, and is a researcher at the Humanoid Robotics Institute (HRI).

J. Santos-Victor is with the Institute for Systems and Robotics, Instituto Superior Técnico, Universidade de Lisboa.

A. Takanishi is with the Department of Modern Mechanical Engineering, Waseda University; and the director of the Humanoid Robotics Institute (HRI), Waseda University.

estimate the real model well, which we prove by validating the energy function on the real robot.

Our focus on energy consumption of humanoid robots is also related to passive walkers [9], which instead of motion planning uses hardware design itself to induce drastic energy efficiency improvements, and other works analysing energy [10] and slippage [6], [11] in robot walking.

### III. PROBLEM STATEMENT

We consider the problem of finding a sequence of  $N$  footsteps  $f_j = (x, y, z, \theta) \in \mathbb{R}^4$ ,  $j = 1, \dots, N$ , such that energy is minimized and approximate reachability, feasibility and slippage constraints are respected. The plan starts at a fixed initial stance  $s_1 = (f_1, f_2)$  and finishes at a fixed goal stance  $s_{N-1} = (f_{N-1}, f_N)$ .  $N$  is unknown;  $(x, y, z)$  and  $\theta$  are position and yaw orientation of a foot in a global coordinate frame; for convenience  $f_j$  is a left foot if  $j$  is odd, right if  $j$  is even. The energetic cost  $E$  of transitioning from a stance  $s_j$  to  $s_{j+1}$  depends on both the stances and some extra parameters  $p \in \mathbb{R}^P$ .  $p$  represents action parameters or controller parameters that might provide different ways for  $s_{j+1}$  to be reached from  $s_j$ , such as step timing and COM motion. In particular in this paper we use  $p = (\Delta t_{ds}, \Delta t_{sw}, \phi_{st}, \phi_{sw}) \in \mathbb{R}^4$  to account for the double-support time (i.e. time spent on  $s_j$ ), swing time (i.e. time spent with the swing leg in the air), and angles of maximum contraction of the stance and swing knees (as parameters to modulate vertical COM motion).

A possible optimization formulation of this problem is

$$\begin{aligned} & \underset{N, f_1 \dots f_N, p_1 \dots p_N}{\text{minimize}} && \sum_{j=2 \dots N-1} E(f_{j-1}, f_j, f_{j+1}, p_j) \\ & \text{subject to} && \\ & R(f_j, f_{j+1}) < 0 && (1) \\ & F(f_{j-1}, f_j, f_{j+1}, p_j) < 0 \\ & S(f_{j-1}, f_j, f_{j+1}, p_j) < \min(\mu_{j-1}, \mu_j, \mu_{j+1}) \\ & a < p_j < b \end{aligned}$$

where the function  $R$  implements constraints on the stances due to robot kinematics,  $F$  implements feasibility constraints on the steps due to kinematic, dynamic or controller limitations, and  $S$  are approximate slippage constraints, where we assume a coefficient of friction  $\mu_j$  is known for each  $f_j$ . Bound constraints on the step parameters are implemented with vectors  $a$  and  $b$ .

### IV. OBTAINING ENERGY, SLIPPAGE, REACHABILITY AND FEASIBILITY MODELS

#### A. Energy

We consider two models of energy consumption, which we compare in the results section. One model is the total mechanical work of the COM of the robot:

$$E_{\text{COM}} = \int_{t_0}^{t_1} |\mathbf{v} \cdot \mathbf{F}| dt. \quad (2)$$

where  $\mathbf{v}$  and  $\mathbf{F}$  are the velocity and total force vectors at the COM, respectively, and  $t_0, t_1$  the beginning and

ending time of a step ( $t_1 - t_0 = \Delta t_{ds} + \Delta t_{sw}$ ). During a training stage we run physics simulations exploring the space of steps  $(f_{j-1}, f_j, f_{j+1}, p_j)$  and collecting energy measurements  $E_{\text{COM}}$ . Using an off-the-shelf machine learning algorithm (Section IV-E) we learn an approximate model

$$\hat{E}(\Delta x_j, \Delta y_j, \Delta z_j, \Delta x_{j+1}, \Delta y_{j+1}, \Delta z_{j+1}, p_j) = E_{\text{COM}}(f_{j-1}, f_j, f_{j+1}, p_j) \quad (3)$$

where  $\Delta x_j$  represents  $x_j - x_{j-1}$  and likewise for  $y$  and  $z$ .

For a DC motor driven robot such as the one we use in the experimental section, we will also compare (2) to the total electrical energy spent by the motors:

$$E_{\text{ele}} = \sum_i \left( \int_{t_0}^{t_1} |\tau_i \omega_i| dt + \int_{t_0}^{t_1} R_i I_i^2 dt \right) \quad (4)$$

where  $i$  is an index of the motor,  $\tau$  is motor torque and  $\omega$  angular velocity.  $I$  refers to current, which in simulation is computed as  $\tau / (r \cdot K_\tau)$ , where  $r$  is the motor's gear reduction ratio and  $K_\tau$  the torque constant.  $RI^2$  are the power losses due to motor armature resistance and we ignore mechanical losses such as joint friction.

#### B. Slippage

As proposed in [6], we enforce slippage constraints at the footstep planning level. We use the maximum ratio of tangential-to-normal force applied at the feet during a given step:

$$S = \max_{t \in [t_0; t_1]} \left| \frac{F_T(t)}{F_N(t)} \right| \quad (5)$$

where  $S$  is called the Required Coefficient of Friction (terminology from human gait literature [12]),  $F_T$  is the tangential force and  $F_N$  normal force at the feet. Note that if  $S$  is lower than the actual coefficient of friction between feet and floor, slippage is prevented during that step.

As with the energy model, we collect  $S$  measurements in physics simulations and use them to train the model:  $\hat{S}(\Delta x_j, \Delta y_j, \Delta z_j, \Delta x_{j+1}, \Delta y_{j+1}, \Delta z_{j+1}, p_j)$ .

#### C. Reachability

We use the same footstep parameterization as in [5] to obtain a heuristic approximation of footstep reachability. In a stance  $s_j$ , reachability is approximated by a set of intervals for the variables  $(\Delta x_{j+1}, \Delta y_{j+1}, \Delta z_{j+1}, \Delta \theta_{j+1})$ , which are distances from the first footstep to the second, i.e.,  $\Delta x_{j+1} = x_{j+1} - x_j$ , etc.

#### D. Feasibility

The simplified reachability heuristic described in Section IV-C does not depend on step parameters  $p$  and may have unmodelled kinematic restrictions and unfeasible regions due to details in lower-level controllers. To avoid unnecessary exploration of footsteps and unfeasible plans, we use an extra feasibility constraint  $F$ . As with energy and slippage models, we collect feasibility measurements from physics simulations and use them to obtain an approximate model. We define  $F \in \{-1, 1\}$  and use value 1 for unfeasible points where the inverse kinematics fails, joint limits are reached or the robot falls, and  $-1$  otherwise.

### E. Implementation

We estimate the energy, slippage and feasibility models by supervised learning of a function  $\hat{f} : \mathbb{R}^{6+P} \rightarrow \mathbb{R}$ , as in (3). In particular, we fit an Infinite Mixture of Linear Experts (IMLE) [13] to the measured simulation data. We choose IMLE due to its high query speed and low number of experts, while still allowing for online learning if necessary. Error performance is comparable to that of gaussian processes [13]. All models mentioned in this paper were trained by uniform sampling of the input space and using the necessary number of experts to obtain a standardized mean squared error (SMSE) lower than 0.1. Models have between 10 and 60 linear experts.

In the case of the feasibility function, we still fit a continuous mixture model eventhough training points are discrete  $F \in \{-1, 1\}$ , leading to interpolation regions between  $-1$  and  $1$ . While planning, we enforce a slightly conservative feasibility constraint of  $F < 0$  to avoid uncertain regions far from feasibility ( $F = -1$ ).

## V. SOLVING THE PLANNING PROBLEM

### A. Discretized search of footsteps, continuous optimization of step parameters

In this paper we solve (1) by a hybrid discrete search and continuous optimization-based planner. We first constrain the footstep (position) space to a point cloud of traversable points  $(x, y, z) \in \mathbb{R}^3$  and a discrete set of orientations in the global coordinate frame:  $\theta \in \{0^\circ, \frac{360^\circ}{D}, \dots, \frac{360(D-1)}{D}^\circ\}$ , where  $D$  is the number of uniform footstep directions. This discrete space is then searched with an anytime A\* search variant: Anytime Repairing A\* (ARA\*) [14].

ARA\* executes a sequence of weighted A\* with state costs  $g(s_j) + wh(s_j)$ .  $g(s_j)$  is the cumulative cost-to-come from the initial stance  $s_1$  to stance  $s_j$ , the heuristic  $h(s_j)$  estimates the cost-to-go from  $s_j$  to the goal stance  $s_{N-1}$ , and  $w \geq 1$  is a weight that trades search speed for optimality (if  $h$  is admissible then solution is optimal for  $w = 1$ ). ARA\* finds a sub-optimal path quickly with a high weight and successively decreases it to improve the path. We compute the energy cost from a stance  $s_j = (f_{j-1}, f_j)$  to  $s_{j+1} = (f_j, f_{j+1})$  as

$$\begin{aligned} \min_{p_j} \quad & E(f_{j-1}, f_j, f_{j+1}, p_j) \\ \text{subject to} \quad & R(f_j, f_{j+1}) < 0 \\ & F(f_{j-1}, f_j, f_{j+1}, p_j) < 0 \\ & S(f_{j-1}, f_j, f_{j+1}, p_j) < \min(\mu_{j-1}, \mu_j, \mu_{j+1}) \\ & a < p_j < b \end{aligned} \quad (6)$$

and define  $E = \infty$  when the problem has no solution. For the cost-to-go heuristic we use an optimistic estimate

$$h(s_j) = \left( \min \frac{E}{d} \right) \cdot d(s_j, s_{N-1}) \quad (7)$$

$$d(s_k, s_l) = \|s_k - s_l\|_{\text{left}(x,y,z)} + \|s_k - s_l\|_{\text{right}(x,y,z)} \quad (8)$$

where  $\|\cdot\|_{\text{left}(x,y,z)}$  (or  $\|\cdot\|_{\text{right}(x,y,z)}$ ) represents the Euclidean distance between  $(x, y, z)$  of the left (or right) foot part of

the stances.  $(\min E/d)$  is a lower bound on step energy per distance. It is pre-computed once as the global minimum of  $d$ -divided (6) including footstep positions as part of the optimization variable.

Note that since ARA\* uses successive weighted relaxations of the heuristic, either the choice of  $w$  or the scale of  $h$  must be chosen appropriately. We keep the algorithm's default sequence of weights, starting at  $w = 5$  and finishing at  $w = 1$  in 0.2 decrements, but normalize all energy costs  $E$  such that the new costs  $E'$  become

$$E' = \frac{V}{\varepsilon} \cdot \left( 1 + \frac{E - \min E}{\max E - \min E} (\varepsilon - 1) \right), \quad (9)$$

where  $V > 0$  is an arbitrarily large positive constant and  $\varepsilon$  is the ratio between the global maximum and minimum of the new scaled costs  $E'$ . Intuitively (9) scales and offsets the step costs  $E$  such that the maximum possible cost is  $\varepsilon$  times greater than the minimum possible cost. We set  $\varepsilon = w = 5$ , corresponding to the largest A\* weight used in the search algorithm. Thus in the initial A\* search with  $w = 5$  we look for a suboptimal plan where each step in a straight line to the goal is expected to have the maximum possible energy (i.e. be the least optimal possible in a straight line). The plan is then successively refined until an optimal solution is found ( $w = 1$ ). In practice we found that such normalization improves the speed of the algorithm in challenging scenarios.

### B. Implementation

We implement point cloud discretization with the PCL library [15] using 5cm grid-filtered point clouds. We also apply a normal filter prior to planning (for simplification in this paper we assume traversable points are horizontal). The search for successors of a stance is done by a range search of 3D points around the fixed foot, and discarding stances heuristically with reachability checks (Section IV-C) before attempting to solve the step optimization problem (6).

We use the official implementation of ARA\* [14] in the Search-Based Planning Library (SBPL) [16]. The optimization problem (6) is solved with the SLSQP algorithm described in [17] and implemented in the NLOpt library [18]. SLSQP is fast and allows arbitrary nonlinear objective and inequality constraints. While its results are theoretically only locally optimal, we did not notice problems with local minima in practice. We always initialize the search variable at the center of the search space. Also note that a faster implementation could be achieved by pre-solving the optimization problem for a large number of footstep and friction conditions.

## VI. RESULTS

All experiments described in this paper were conducted on the human-size humanoid robot WABIAN [19].

### A. Simulated models of energy, slippage and feasibility

We generated 11,519 different walking patterns exploring the input space of the models. Each pattern is a sequence of 6 steps stabilized with a ZMP-based controller [20] and simulated on the ODE physics simulator, 4ms control cycle.

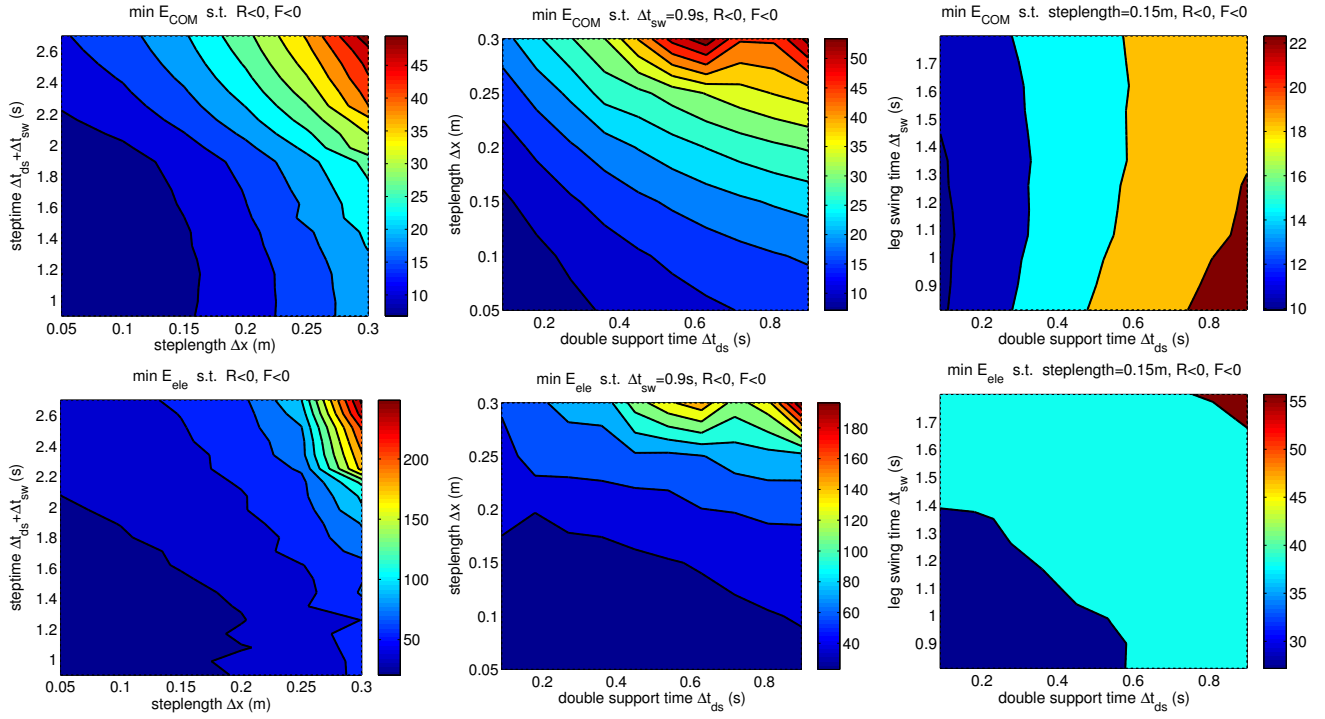


Fig. 1. Minimum COM energy  $E_{COM}$  (top) and simulated electrical energy  $E_{ele}$  (bottom) measured in physics simulation.

Joints are position controlled. Full trajectories of the knees were obtained by spline interpolation between stretch (1 degree) at impact, and bend ( $\phi_{st}$ ,  $\phi_{sw}$ ) just after double support. ZMP references were set on the center of the stance foot during the swing phase, and spline-interpolated to the other foot during the double support phase.

From these simulations we gathered measurements of  $E_{COM}$ ,  $E_{ele}$ ,  $S$  and  $F$ . The limits of stance reachability (Section IV-C) were set according to the dimensions and approximate kinematics of WABIAN by manual inspection:

- $\Delta x \in [0; 0.38]$  meters, where  $x$  points forward,
- $\Delta y \in [0.17; 0.30]$  meters, where  $y$  points to the left (symmetric interval if  $f_{j+1}$  is a right foot),
- $\Delta z \in [-0.15; 0.15]$  meters, where  $z$  point upward,
- $\Delta \theta \in [0; 30]$  degrees, where  $\theta$  runs counter-clockwise (symmetric interval if  $f_{j+1}$  is a right foot),

and step parameters  $p$  were sampled within the intervals:

- $\Delta t_{ds} \in [0.09; 0.9]$ ;  $\Delta t_{sw} \in [0.9; 1.8]$  seconds,
- $\phi_{st} \in [5; 45]$ ;  $\phi_{sw} \in [5; 45]$  degrees.

Figure 1 shows the COM energy model  $E_{COM}$  and simulated electrical energy model  $E_{ele}$ . The results are for forward walking patterns. Step-length represents the quantity  $\Delta x_j = \Delta x_{j+1}$  (e.g. a step-length of 30cm is a step taken from a 30cm-long stance to another 30cm-long stance) and step time represents  $\Delta t_{ds} + \Delta t_{sw}$ . The figures show that the contours of  $E_{COM}$  are similar to  $E_{ele}$ , suggesting that optimization of the simpler  $E_{COM}$  could be sufficient. For both energy definitions there is a clear global optimum of energy in step length and time. Also, most of the energy is consumed in the double support phase: the shorter  $\Delta t_{ds}$  the lower the

energy. One important difference between the models is that leg swing time mostly does not influence COM energy. This is because the COM and stance leg have near zero velocity during swing. Electrical energy, since it considers the squared torques on the (zero velocity) stance leg, accounts for the energy being spent to support the COM with the knee and ankle joints. Hence the deformed graph of  $E_{ele}(\Delta t_{ds}, \Delta t_{sw})$  when compared to  $E_{COM}(\Delta t_{ds}, \Delta t_{sw})$ . It is also interesting to analyse the energy spent per distance traveled (i.e. per step-length). Figure 2 shows the minimum  $E_{COM}$  per distance depending on step-length and time, where the optimal step-length is around 0.15m (i.e. 0.30m stride).

Figure 2 also shows the slippage and feasibility models. Slippage  $S$  is the same as presented in [6], where it is referred to as a "required coefficient of friction" model. For a more in-depth analysis please refer to [6]. The figure shows that when walking on very slippery terrain, step-length and double support time can be optimized such as to avoid slippage. To achieve lower values of tangential-to-normal force and walk on more slippery terrain, the robot should increase double support time and/or shorten the steps. The feasibility model is shown as a function of the knee angles  $\phi_{st}$ ,  $\phi_{sw}$  used to control vertical COM motion. Points between feasibility  $F = -1$  and unfeasibility  $F = 1$  were interpolated.

### B. Energy comparison: simulated vs real robot

We ran a small subset of experiments on the real robot to compare real electrical energy  $E_{ele}^*$  to the simulated  $E_{ele}$  model. Figure 3 shows the simulated optimal  $E_{COM}/\text{steplength}$  and  $E_{ele}/\text{steplength}$  for each step-length, varying all other step parameters. We also show the real

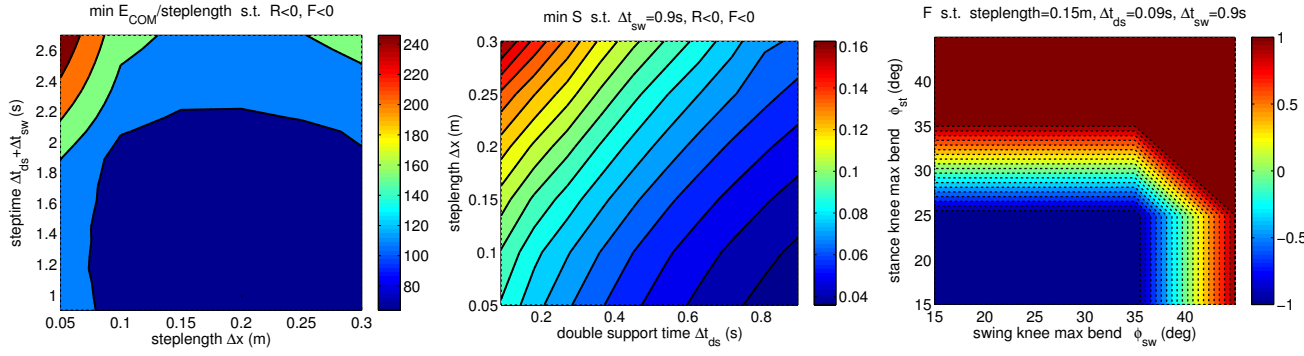


Fig. 2. Left: Minimum COM energy  $E_{COM}$  per distance traveled. Middle: Slippage  $S$ , or the maximum ratio of tangential-to-normal force over a step. It indicates the minimum ground coefficient of friction  $\mu$  where the robot can walk without slipping. Right: Feasibility  $F$  for fixed step length and timing.  $F = -1$  is feasible, 1 unfeasible, points inbetween are interpolated. A point is considered feasible if during a step the inverse kinematics are feasible, joint limits respected and the robot does not fall.

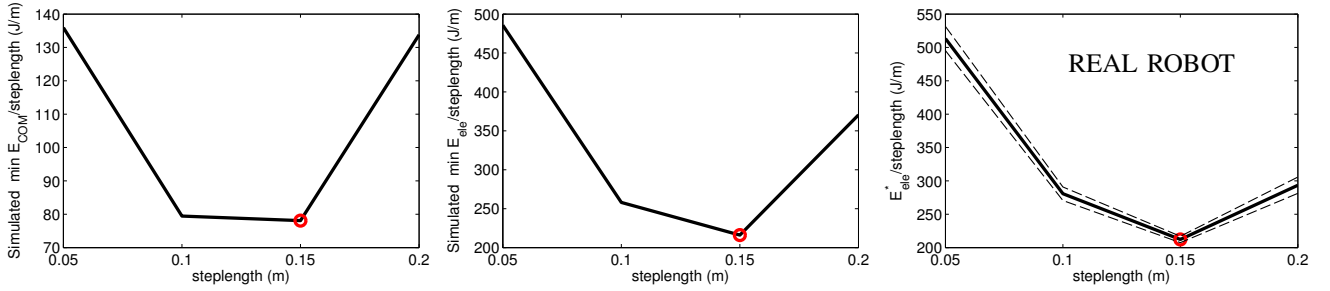


Fig. 3. Simulated versus real energy consumption. Mechanical energy  $E_{COM}$  (left), simulated electrical energy  $E_{ele}$  (middle) and measured electrical energy  $E_{ele}^*$  (right). The real energy curve was obtained by averaging over 18 steps for each step-length and standard deviation is also shown.

measured  $E_{ele}^*/\text{steplength}$  in the same figure for comparison. To obtain  $E_{ele}^*$  we made the robot walk in the laboratory for a total of 18 steps for each step-length value (using the energy-optimal step parameters obtained from simulated models). We used motor current measurements given by the motor drivers, and computed torques from the current measurements as well. Each point in the graph is the average energy over the 18 steps. The standard deviation of the measurements is also shown in the same figure. The minimum energy per distance is obtained at the same step-length of 0.15m for all models (i.e. 0.30m stride length). The standard deviation of the energy measurements on the real robot is low, especially at the optimum, which we believe to be due to higher stability as well. The figure also shows that COM mechanical energy  $E_{COM}$  overestimates energy consumption after the minimum, and that this overestimation is lower in case a more complex model is used (i.e. joint work plus a  $\tau^2$  term). Figure 4 shows one of the real robot experiments taken at optimal step-length.

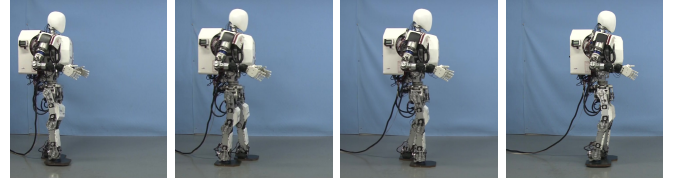


Fig. 4. Real robot walking with optimal parameters (red dot in Fig. 3).

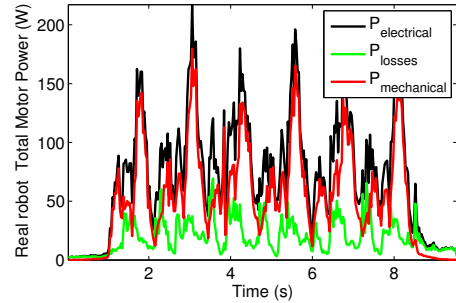


Fig. 5. Real total electrical power measured over a 6-step trial.  $P_{electrical} = P_{mechanical} + P_{losses}$ .

To observe the impact of mechanical energy and heat losses in  $E_{ele}^*$ , we also show in Figure 5 the total electrical power across a 6-step experiment. We decompose power into joint mechanical power (first term of equation 4) and power losses (second term of equation 4). Mechanical power dominates power consumption over heat losses of the DC motors, and closely follows the total energy of the system. This agrees with the other results, in that optimizing mechanical

work might be sufficient for good energy consumption of the robot.

### C. Optimal planning

We applied the described planner to two different scenarios using  $E_{COM}$  as the objective function. Reported energy

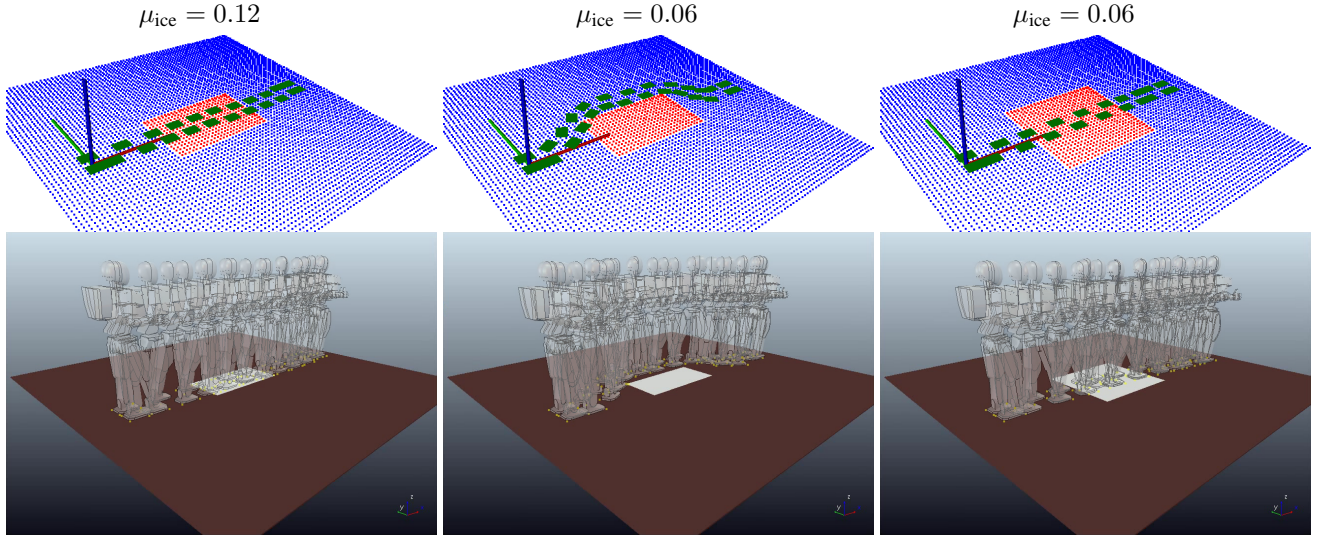


Fig. 6. Optimal plans obtained by our planner in the “ground and ice-patch” scenario. The top row shows the footstep plan and point cloud (red has friction  $\mu_{ice}$ , blue  $\mu_{ground} = 1$ ). Left: robot crosses a narrow ice patch ( $\mu_{ice} = 0.12$ ). Middle: robot walks around the patch if its slipperiness is increased ( $\mu_{ice} = 0.06$ ). Right: robot walks slowly through the same ice patch in case the ice is wider (energy spent avoiding it would be too high).

results are the resultant  $E_{ele}$ . The first scenario (Figure 6) is as follows: the robot stands in a ground with friction  $\mu_{ground} = 1.0$  and has to walk to a target 3m away, straight. Between the start and finish points there is an “ice patch” of very low friction  $\mu_{ice}$ . We conducted several planning experiments with different  $\mu_{ice} = \{0.12, 0.06\}$  and different widths of the the ice patch ( $\{0.5, 1\}$ m). Figure 6 shows that the robot walked through the ice for  $\mu_{ice} = 0.12$  but walked around it if  $\mu_{ice} = 0.06$ . Specifically it walked 5% slower than the normal speed when on the ice patch, to avoid slipping ( $S < \mu$  constraint). When we doubled the ice patch width but kept the low friction  $\mu_{ice} = 0.06$ , the planner found it more optimal to go slower through the ice than around a great distance. We show the total energy cost of each plan in Table I.

We also computed the energy cost of a sub-optimal plan: one which forces the robot to avoid the ice patch when it is optimal to cross it, or vice-versa. To obtain such plans we used the same planner but constrained the environment to force the opposite choice (i.e. treating the ice as an obstacle or widening the ice). The results show that our optimal path is between 10 and 19% more energy efficient than the sub-optimal choice. With non-optimized code (optimization problem (6) is solved for each expanded node), the planner found a first sub-optimal path in around 8 seconds and the final path in around 10 minutes.

The second scenario (Figure 7) is as follows: there are two stairs at equal distance to the robot ( $x = 1$  meter away,  $y = \pm 0.50$ m), both ending at the same final height ( $z = 0.50$ m). One of the stairs has 3 high steps while the other has 6 lower steps. The goal of the robot is to reach a distant centered position  $(x, y, z) = (3, 0, 0.5)$ m. The energy cost should be the same if the stairs were identical. Figure 7 shows that the planner opts for the lower-but-many-step stairs. The total energy spent is 9% lower than if the few-but-high-step stairs

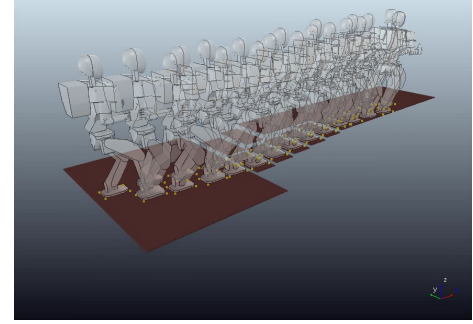


Fig. 7. Optimal plan obtained by our planner in the “two stairs” scenario.

TABLE I  
ELECTRICAL ENERGY CONSUMPTION OF OPTIMAL AND SUBOPTIMAL PLANS

	Optimal energy (our planner)	“Sub-optimal choice”*	Energy saved
narrow ice $\mu = 0.12$	2110 J	2427 J	14%
narrow ice $\mu = 0.06$	2427 J	3031 J	19%
wide ice $\mu = 0.06$	3031 J	3384 J	10%
stairs $\mu = 1$	4116 J	4535 J	9%

\*Note: “Sub-optimal choice” refers to a sub-optimal plan that takes the alternative option (i.e. around the ice instead of through; through instead of around; or using the few-but-high-step stairs) although still with optimal steps for that constraint.

were chosen (see Table I). With non-optimized code, the planner found a first sub-optimal path in 130 seconds and the final path in around 10 minutes. This experiment shows that the robot has an energy-optimal step height: after a certain height, steps become too costly for the distance travelled.

## VII. DISCUSSION

**Mechanical energy vs heat losses.** In our experiments, mechanical energy (torque times velocity term) dominated over energy losses on the motor armature resistance (current



or torque squared term) and also mechanical COM energy approximated total electrical energy. This is not a general result to all humanoid, but one that may be considered if the robot is DC-motor driven with high gear ratios (WABIAN's are 200) and uses a stretched-knees walking controller, which can decrease torques on the knee joints [21]. A bent-knees controller, on the other hand, where COM height is fixed throughout the walk, could lead to higher average torques at the knee joints, making energy losses higher.

**Feasibility model.** The use of a feasibility model learned in simulation was crucial in our experiments. One of the problems of the contact-before-motion planning paradigm is to generate a contact plan for which whole-body motion is feasible. In practice we found heuristic limits on stance distances to be insufficient to obtain feasible plans due to two reasons: unmodeled kinematics (e.g. a large step is possible only if the COM height is below a certain limit), and dynamic unfeasibility (e.g. the low-level controller might be unstable for a certain region of the space). Using a learned  $F$  as a constraint alleviated this problem and speeded up planning considerably since more stances and steps were discarded early on. Using this approach, we had no problems with falls or joint limits being reached.

**Improving planner speed.** For the results in this paper, optimization problem (6) was solved for each expanded node in the A\* search. While the plans were still obtained reasonably fast (8 seconds for the first sub-optimal plan), performance could be increased considerably by learning an auxiliary function whose value is the solution of (6) for a given  $\mu$ . Then, each expanded node only queries  $E$  once, and step parameters  $p$  can be computed on the final plan.

## VIII. CONCLUSIONS

In this paper we showed that optimal planning of humanoid robot locomotion, in terms of energy, feasibility and slippage, is possible at the footstep level. We extended the notion of footstep planning to placement, timing and parameterized COM motion. We measured how energy of the humanoid WABIAN varies with such parameters in simulation and used the resulting models to minimize energy consumption during walking. We also obtained models of slippage (tangential over normal force) and feasibility (joint limits and falls) used as constraints in the energy minimization problem to guarantee slippage- and fall-free paths.

The results of planning experiments show that our models and A\*-integration allow the robot to optimally deal with the presence of slippery surfaces and different climbing gradients (stair dimensions), saving between 9 and 19% energy when compared to a suboptimal planner that, for example, avoids slippery terrain or chooses more energy-consuming stairs.

Our experiments also showed that minimizing the simulated energy models leads to minimal energy consumption on the real robot as well and that, at least for our robot and stretched-knees walking controller, minimizing mechanical work of the joints or, even simpler, the COM, is sufficient for good energy efficiency.

## REFERENCES

- [1] R. Deits and R. Tedrake, "Footstep planning on uneven terrain with mixed-integer convex optimization," in *14th IEEE-RAS International Conference on Humanoid Robots*, Nov 2014, pp. 279–286.
- [2] W. Huang, J. Kim, and C. Atkeson, "Energy-based optimal step planning for humanoids," in *2013 IEEE International Conference on Robotics and Automation*, May 2013, pp. 3124–3129.
- [3] J. Chestnutt, M. Lau, G. Cheung, J. Kuffner, J. Hodgins, and T. Kanade, "Footstep planning for the honda asimo humanoid," in *2005 IEEE International Conference on Robotics and Automation*, April 2005, pp. 629–634.
- [4] J. Garimort and A. Hornung, "Humanoid navigation with dynamic footstep plans," in *2011 IEEE International Conference on Robotics and Automation*, May 2011, pp. 3982–3987.
- [5] A. Hornung, A. Dornbush, M. Likhachev, and M. Bennewitz, "Any-time search-based footstep planning with suboptimality bounds," in *12th IEEE-RAS International Conference on Humanoid Robots*, Nov 2012, pp. 674–679.
- [6] M. Brandao, K. Hashimoto, J. Santos-Victor, and A. Takanishi, "Gait planning for biped locomotion on slippery terrain," in *14th IEEE-RAS International Conference on Humanoid Robots (Humanoids)*, November 2014, pp. 303–308.
- [7] J. Kim, N. Pollard, and C. Atkeson, "Quadratic encoding of optimized humanoid walking," in *13th IEEE-RAS International Conference on Humanoid Robots*, Oct 2013, pp. 300–306.
- [8] N. Perrin, O. Stasse, L. Baudouin, F. Lamiraux, and E. Yoshida, "Fast humanoid robot collision-free footstep planning using swept volume approximations," *IEEE Transactions on Robotics*, vol. 28, no. 2, pp. 427–439, April 2012.
- [9] S. Collins and A. Ruina, "A bipedal walking robot with efficient and human-like gait," in *2005 IEEE International Conference on Robotics and Automation*, April 2005, pp. 1983–1988.
- [10] F. Silva and J. Machado, "Energy analysis during biped walking," in *1999 IEEE International Conference on Robotics and Automation*, vol. 1, 1999, pp. 59–64 vol.1.
- [11] S. Kajita, K. Kaneko, K. Harada, F. Kanehiro, K. Fujiwara, and H. Hirukawa, "Biped walking on a low friction floor," in *2004 IEEE/RSJ International Conference on Intelligent Robots and Systems*, vol. 4, Sept 2004, pp. 3546–3552 vol.4.
- [12] R. Cham and M. S. Redfern, "Changes in gait when anticipating slippery floors," *Gait & Posture*, vol. 15, no. 2, pp. 159 – 171, 2002.
- [13] B. Damas and J. Santos-Victor, "Online learning of single- and multi-valued functions with an infinite mixture of linear experts," *Neural computation*, vol. 25, no. 11, pp. 3044–3091, 2013.
- [14] M. Likhachev, G. J. Gordon, and S. Thrun, "Ara\*: Anytime a\* with provable bounds on sub-optimality," in *Advances in Neural Information Processing Systems*, 2003, p. None.
- [15] R. B. Rusu and S. Cousins, "3D is here: Point Cloud Library (PCL)," in *2011 IEEE International Conference on Robotics and Automation*, Shanghai, China, May 9-13 2011.
- [16] M. Likhachev. (2010) Search-based planning library. [Online]. Available: <http://www.ros.org/wiki/sbpl>
- [17] D. Kraft, "Algorithm 733: Tomp-fortran modules for optimal control calculations," *ACM Transactions on Mathematical Software*, vol. 20, no. 3, pp. 262–281, Sep 1994.
- [18] S. G. Johnson. The nlopt nonlinear-optimization package. [Online]. Available: <http://ab-initio.mit.edu/nlopt>
- [19] Y. Ogura, H. Aikawa, K. Shimomura, H. Kondo, A. Morishima, H. Lim, and A. Takanishi, "Development of a new humanoid robot wabian-2," in *2006 IEEE/RSJ International Conference on Robotics and Automation*. IEEE-RAS, 2006.
- [20] Y. Ogura, T. Kataoka, K. Shimomura, H.-o. Lim, and A. Takanishi, "A novel method of biped walking pattern generation with predetermined knee joint motion," in *2004 IEEE/RSJ International Conference on Intelligent Robots and Systems*, vol. 3. IEEE, 2004, pp. 2831–2836.
- [21] Y. Ogura, T. Kataoka, H. Aikawa, K. Shimomura, H. ok Lim, and A. Takanishi, "Evaluation of various walking patterns of biped humanoid robot," in *2005 IEEE International Conference on Robotics and Automation*, April 2005, pp. 603–608.